Supplemental Material
Critical yielding rheology: from externally deformed glasses to active systems

Carlos Villarroel[1], Gustavo Düring[1,2]
[1] *Instituto de Física, Pontificia Universidad Católica de Chile, Casilla 306, Santiago, Chile*
[2] *ANID - Millenium Nucleus of Soft Smart Mechanical Metamaterials, Santiago, Chile*

(Dated: September 29, 2021)

Simulation protocols.

Here we give more details about the simulation protocols and how the data analysis is done for both models. In SS models, like the one proposed by Durian [1], a speed profile is generally imposed with a given shear rate $\dot{\gamma}$ value, and as a consequence, the value of σ is measured as the temporal average over a sufficiently long simulation time. In SRF model, we distinguish two different kind of algorithm [2], the first at constant self-force (SRF-CSF), where the value of f remains fixed throughout the simulation, and the second at constant parallel velocity (SRF-CPV), where the value $v_{\parallel}^{R} = \frac{1}{N}\sum \vec{v}_i \cdot \vec{n}_i^{R}$ is set, and in each step the value of f is adjusted to keep $v_{\parallel}^{R}$ constant. The SRF-CPV method has the advantage of allowing exploration closer to the critical point. This is because, similarly to what happpens in systems under shear, it is possible for the system to find equilibrium for $f > f_c$ due to finite size effects [3, 4]. In this line, the SRF-CPV method ensures a flow that does not suddenly stagnate in the vicinity of f_c. In Fig. 1 we show that the choice of simulation method does not change the results in areas where sudden stagnation is not observed.

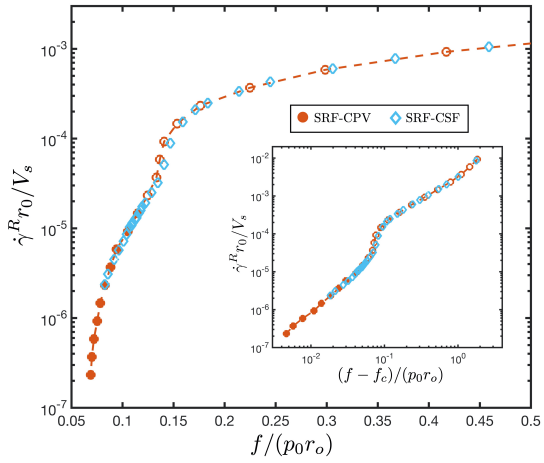

FIG. 1. $\dot{\gamma}^R$ vs. f using SRF-CPV and SRF-CSF (section without effects of finite size) for $N = 16384$, $\phi = 0.925$ and harmonic potential. It is observed that both curves show the same behavior.

One last point to discuss is how the value of σ_c and f_c are calculated. For SS and SRF-CPV, the values are calculated by fitting the HB curve and looking for the values of σ_c and f_c that maximize χ^2, respectively. In the case of SRF-CSF, a sweep is made in f values, with a jump of $\Delta f = 0.00005$, and f_c is set for the highest value at which stagnation is appreciated. We also verify that calculation of f_c is independent of the simulation method.
To simulate the system dynamics, the time is measured in units of $t_0 = r_0^2/D\epsilon$, and we integrate the overdamped particle equation using the RK-2 method at each time step. Unless otherwise specified, we use two system sizes $N = 16384$ and $N = 65536$ with $\Delta t = 0.85 t_0$, where we have verified that the selection of Δt does not affect results. For all our results using the SS model, average is taken over 20 different configurations, and for all our results using the SRF model, average is taken over 96 different configurations.

Irving-Kirkwood

To quantify pressure and shear stress we use the Irving-Kirkwood calculation [5] for the stress tensor $\sigma_{\alpha\beta}$. We do this to avoid neglecting the effects of free particles that may be present in gaseous areas.

$$\sigma_{\alpha\beta} = \frac{1}{V}\left(\sum_{i<j} \vec{r}_{ij,\alpha}\vec{f}_{ij,\beta} + \sum_i \delta\vec{v}_{i,\alpha}\delta\vec{v}_{i,\beta}\right). \qquad (1)$$

In this equation, the indices α and β are the cartesian coordinates, $\vec{f}_{ij}$ and $\vec{r}_{ij}$ are vector force and vector distance between the particles, $\delta\vec{v}_i$ are the fluctuations around the mean parallel velocities, which we define as $\delta\vec{v}_i = \vec{v}_i - \dot{\gamma}(\vec{r}_i \cdot \hat{y})\hat{x}$ for SS and $\delta\vec{v}_i = \vec{v}_i - v_{\parallel}\hat{n}_i^R$ for SRF. With these expressions, we seek to cancel out the contributions of the deformations to the velocity $\vec{v}_i$. In order to do this in the SS model, we need only to subtract the speed profile term. On the other hand, for the SRF model, we know that the effect of the self-force will lead to each particle moving with an mean velocity $v_{\parallel}$; for this reason, we consider that the vectorial term that provides the deformation can be written as $v_{\parallel}\hat{n}_i^R$. Shear stress σ is defined as $\sigma \equiv \sigma_{xy}$, and the pressure as $p \equiv (\sigma_{xx}+\sigma_{yy})/2$.

f_c at infinity system size.

Here, we do a finite-size analysis, which is essential to validate the existence of an active yielding transition in the thermodynamic limit $f_c(\phi, N \to \infty)$. Using the SRF-CSF, we calculate how the value of f_c depends on N. These results are shown in image Fig.2a, where it can be seen that the value of f_c saturates at a value f_c^∞ in the limit $N \to \infty$.

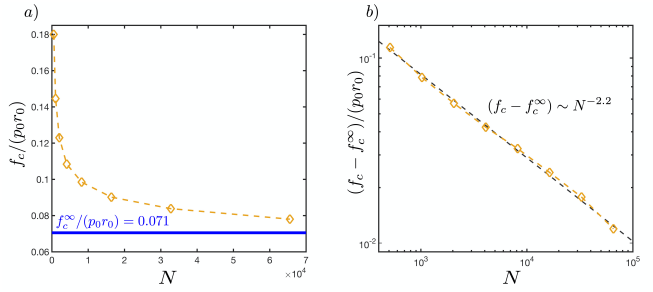

FIG. 2. For $\phi = 0.925$ and harmonic potencial: a) f_c vs. N, the data appears to converge to $f_c^\infty/p_0 r_0 = 0.071$. b) $f_c - f_c^\infty$ vs. N, the data shows a power law $(f_c(N) - f_c^\infty) \sim N^{-2.2}$.

For our simulation with $\phi = 0.925$, $f_c^\infty/p_0 r_0 = 0.071$ is obtained, and a power law $(f_c(N) - f_c^\infty) \sim N^{-2.2}$ is appreciated (see Fig. 2b). The existence of a non-zero value of f_c^∞ suggests that the presence of an active yielding transition is not a finite size problem.

Phase separation detection.

A second detection method, which requires less computational effort, is based on the idea that when nucleation is present, the effective area A_{eff} occupied by the particles in liquid areas decreases, which causes an increase in the global pressure p. For the calculation of the effective area A_{eff}, a tessellation algorithm on free space is used (see Fig. 3), adjusted to have a maximum error of 1.5%. The Fig. 4a shows how p evolve over the simulation time.

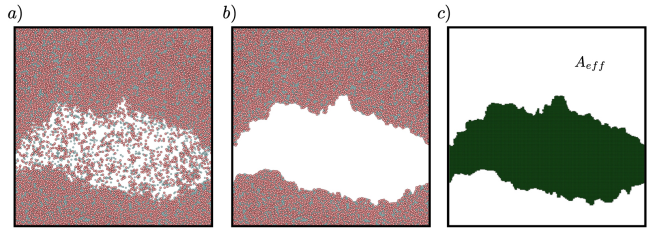

FIG. 3. Tessellation algorithm scheme for $N = 16384$, $\phi = 0.925$: a) system that exhibits a nucleation zone; b) system where all particles with less than three contacts were removed, effectively removing the gaseous zone from the system; c) the area where the removed particles were (in green) is computed using the tessellation algorithm, and this is used to calculate the effective area A_{eff}.

In Fig. 4b,c we see how, for values of $f > f^\star$, there are sudden increases in pressure p which overlap with a decrease in A_{eff}. In our data, we consider that a system does not show phase separation when, for a given value of f, it satisfies the condition $p/p_0 < 1.05$ for all configurations at all simulation times.

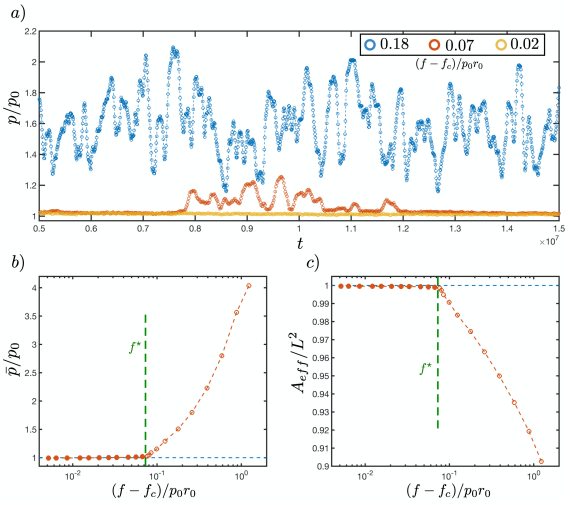

FIG. 4. For $N = 16384$, $\phi = 0.925$ and harmonic potential: a) Pressure p vs. simulation time t. For $(f - f_c)/p_0 r_0 = 0.02$, no increase in pressure is observed (homogeneous liquid). For $(f - f_c)/p_0 r_0 = 0.07$ an increase in pressure is observed in some instances (there are some configurations where nucleation occurs). For $(f - f_c)/p_0 r_0 = 0.18$, an increase in pressure is observed for all simulation times (all configurations show nucleation). b) Mean pressure $\bar{p}$ vs. $(f - f_c)/p_0 r_0$. c) Effective area A_{eff} vs. $(f - f_c)/p_0 r_0$.

Shear oscillation.

The existance of a correlation time related to the structure's lifetime can also be verified using oscillation simulations for the SS model. Here we invert the orientation of the velocity profile $\dot{\gamma} \to -\dot{\gamma}$, which causes a change in the measured stress value $\sigma \to -\sigma$ (see Fig. 5). Due to the presence of these structures, the jump between σ and $-\sigma$ is not instantaneous, so we define the lifetime of the structures t^* as the time necessary for this change in the stress value to occur.

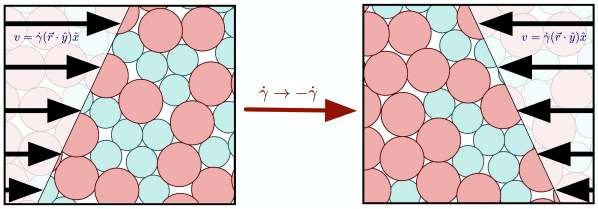

FIG. 5. Shear oscillation scheme. The orientation of the velocity profile changes abruptly ($\dot{\gamma} \to -\dot{\gamma}$).

The Fig. 6a shows how this process is carried out. Firstly, the system is subjected to a shear rate $\dot{\gamma}$, and as a result, the stress varies around an average value $\bar{\sigma}$. Then, in time t_i, the orientation changes abruptly to $-\dot{\gamma}$, and we wait until the value $-\bar{\sigma}$ is reached in time t_f. In Fig. 6b we show how $t^* = t_f - t_i$ depends on $\dot{\gamma}$,which verifies that the lifetime of the structures in the SS simulations follows a power law $t^* \sim \dot{\gamma}^{-0.93}$.

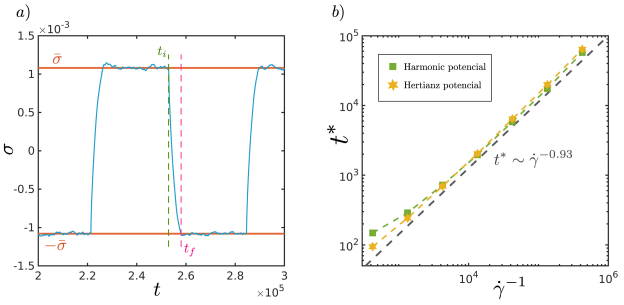

FIG. 6. For shear oscillation method: a) Shear stress σ vs. simulation time t for $N = 65536$ and $\dot{\gamma} = 3.2 \times 10^{-5}$; shear stress changes its orientation from $\bar{\sigma}$ to $-\bar{\sigma}$ between times t_i and t_f. b) t^* vs. $\dot{\gamma}^{-1}$ for $N = 65536$ and both potentials, a power law $t^* \sim \dot{\gamma}^{-0.93}$ is obtained.

[1] D. J. Durian, *Phys. Rev. Lett.*, 1995, **75**, 4780–4783.
[2] R. Mo, Q. Liao and N. Xu, *Soft Matter*, 2020, **16**, 3642–3648.
[3] A. H. Clark, J. D. Thompson, M. D. Shattuck, N. T. Ouellette and C. S. O'Hern, *Phys. Rev. E*, 2018, **97**, 062901.
[4] N. Xu and C. S. O'Hern, *Phys. Rev. E*, 2006, **73**, 061303.
[5] J. H. Irving and J. G. Kirkwood, *The Journal of Chemical Physics*, 1950, **18**, 817–829.